CALCULATION OF OPTICAL FUNCTIONS OF EXCITON AND ELECTRON TRANSITIONS BY MEANS OF KRAMERS-KRONIG RELATIONS IN CuAlS$_2$ CRYSTALS

I. G. Stamov[1], N. N. Syrbu[2], B. V. Korzun[3], V. V. Ursaki[4], A. V. Dorogan[2], and A. Masnik[2]

[1]*Tiraspol State Corporative University, Lablocikin str. 5, Tiraspol, MD-2069 Republic of Moldova*
[2]*Technical University of Moldova, Stefan cel Mare pr. 168, Chisinau, MD-2004Republic of Moldova*
[3]*Institute of Physics of Solids and Semiconductors, Brovki 17, Minsk, 220072 Republic of Belarus*
[4]*Institute of Applied Physics, Academy of Sciences of Moldova, Academiei str. 5, Chisinau, MD-2028 Republic of Moldova*

Abstract

Excitonic reflection spectra of CuAlS$_2$ crystals were measured at a temperature of 10 K for $E//c$ and $E\perp c$ polarizations. The shapes of the lines of ground states of Γ_4 and Γ_5 excitons were calculated by means of the Kramers-Kronig relations. Exciton parameters and the values of energetic gaps (Γ_7–Γ_6, Γ_6–Γ_6, and Γ_7–Γ_6) were determined. Optical reflection spectra in the depth of absorption band (E$_g$ - 6 eV) were measured at 80 K for $E//c$ and $E\perp c$ polarizations. Optical functions n, k, ε_1, ε_2, $d^2\varepsilon_1/dE^2$ and $d^2\varepsilon_2/dE^2$ were calculated for both polarizations. The revealed peculiarities are ascribed to electronic transitions in the frame of theoretical calculations of the band structure for crystals from this group.

1. Introduction

The CuAlS$_2$ compound, which belongs to I–III–VI$_2$ group, crystallizes into a chalcopyrite structure with a spatial group $I_{2d}^4 - D_{2d}^{12}$ and has the widest band. There is great interest in the crystals of this group (I–III–VI$_2$) because of the expected applications in optoelectronic devices. Solar energy converters are successfully elaborated on the basis of materials of this group. Thin film devise structures were prepared on the basis of some of these compounds [1, 2]. The energy band structure of chalcopyrites was calculated as most close analogs of binary compounds with a zincblende structure (ZnSe, ZnS) [3–6]. All the crystals of I–III–VI$_2$ group possess a strong anisotropy of optical properties in the region of fundamental absorption [7, 13]. Many chalcopyrite compounds, including CuAlS$_2$, were prepared in the form of epitaxial layers by means of molecular beam epitaxy [14].

In this paper, the optical spectra of CuAlS$_2$ crystals are studied in the excitonic region. The line-shape of ground Γ_4 and Γ_5 exciton states in the reflection spectra are calculated by means of the Kramers-Kronig relations. Optical functions n, k, ε_1, ε_2, $d^2\varepsilon_1/dE^2$ and $d^2\varepsilon_2/dE^2$ were calculated for $E//c$ and $E\perp c$ polarizations from the measured optical reflection spectra in the depth of absorption band (E$_g$ − 6 eV). The revealed peculiarities are ascribed to electronic transitions in the frame of

theoretical calculations of the band structure.

2. Experimental

CuAlS$_2$ crystals in the form of plates with mirror surfaces of 2.5 x 8 mm^2 and thickness of 1–2 mm were grown by chemical vapor transport in ampoules. The surfaces of some plates are parallel to the C axis. Reflection spectra in the region of Γ_4 and Γ_5 excitons were measured using an MRD-2 spectrometer, while the optical spectra in the depth of absorption band were investigated by means of a SPECORD-M40 spectrometer. For low-temperature measurements, the samples were mounted on the cold station of an LTS-22 C 330 optical cryogenic system.

3. Experimental results and discussion

According to theoretical calculations of the band structure [3–6], the minimum of interband gap is formed by direct electronic transitions at the center of Brillouin zone for CuAlS$_2$ crystals. The lower conduction band possesses Γ_6 symmetry and the upper valence bands V$_1$, V$_2$, V$_3$ possess Γ_7, Γ_6 and Γ_7 symmetries, respectively. The interaction of electrons from the conduction band Γ_6 with holes from Γ_7 is determined by the product of irreducible representations Γ_1 x Γ_6 x $\Gamma_7 = \Gamma_3 + \Gamma_4 + \Gamma_5$. As a result of this interaction, the Γ_4 exciton allowed in E∥c polarization, Γ_5 exciton allowed in E⊥c polarization and Γ_3 exciton forbidden in both polarizations are formed in the long-wavelength part of the spectrum. The interaction of electrons from the conduction band C$_1$ of Γ_6 symmetry with holes from the valence band V$_2$ with Γ_6 symmetry leads to the appearance of three excitonic series Γ_1, Γ_2, and Γ_5. According to the selection rules, Γ_5 excitons are allowed, while Γ_1 and Γ_2 excitons are forbidden for E⊥c polarization.

The lines $n = 1$ ($\omega_t = 3.543$ eV, $\omega_L = 3.546$ eV) and $n = 2$ (3.565 eV) of the hydrogen-like Γ_4 exciton series were revealed in the reflection spectra of CuAlS$_2$ crystals measured at 10 K in E∥c polarization [7]. The reflection spectra in the n = 1 region has a typical form with a 3.543 eV maximum and a 3.546 eV minimum. These peculiarities are explained by the presence of transversal and longitudinal excitons. The longitudinal-transverse splitting energy of Γ_4 excitons estimated on the basis of these data equals 3 meV. A Rydberg constant of 32 meV is determined for Γ_4 excitonic series from the energetic position of $n = 1$ and $n = 2$ lines (fig. 1). The continuum energy (E_g, $n = \infty$) is 3.575 eV. The energy values discussed above for the ground ($n = 1$) and excited ($n = 2$) excitonic states are satisfactorily correlating with the 3.534 eV and 3.665 eV values previously obtained at 77 K [8].

A maximum at 3.668 eV (transversal exciton) and a minimum at 3.670 eV (longitudinal exciton) related to Γ_5 excitonic series are revealed in E⊥c polarization (Fig. 1). The transverse-longitudinal splitting of Γ_5 exciton equals 2.0 meV. An excited state $n = 2$ is revealed at 3.687 eV. The exciton binding energy of Γ_5 excitons is 25 meV, and the convergence limit of the series is 3.693 eV. The C exciton is revealed at 3.813 eV (n=1) in the same polarization [7]. The reflection coefficient for the B-excitonic series is 21% at 3.6 eV, and the dielectric constant ε_b is 7.2. A value of the effective mass μ equal to 0.09m$_o$ is derived for a binding energy of 25 meV.

The phase φ of the reflected beam and the magnitude of the absorption coefficient K in the resonance region of Γ_4 and Γ_5 excitons are obtained from the calculations of reflection spectra by means of Kramers-Kronig relations (Fig. 1). It is known that the amplitude of the reflection coefficient R is related to the phase φ of the reflected beam according to the following expression:

$$r = \sqrt{R}e^{-i\varphi} \tag{1}$$

The optical functions n, k, R, φ, ε_1, ε_2 are related to each other by the following correlations:

$$\begin{cases} r = \dfrac{N-1}{N+1} = \dfrac{n+ik-1}{n+ik+1} \\ r = \sqrt{R}e^{-i\varphi} = \sqrt{R}(\cos\varphi - i\sin\varphi) \end{cases} \Rightarrow \begin{cases} n = \dfrac{1-R}{1-2\sqrt{R}\cos\varphi + R} \\ k = \dfrac{2\sqrt{R}\sin\varphi}{1-2\sqrt{R}\cos\varphi + R} \end{cases} \tag{2}$$
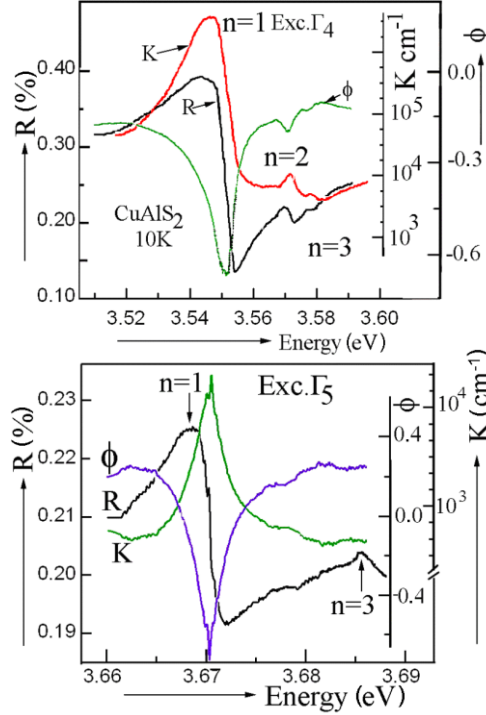

Fig. 1. Spectral dependence of absorption coefficient (K) and of phase (Φ) of the reflected beam calculated from the measured reflection spectra (R) in CuAlS$_2$ crystals.

The phase $\varphi \approx \varphi(\omega)$ is calculated for each wavelength value by using the Kramers–Kronig integrals on the basis of experimentally measured amplitude values of the reflection coefficient $R \approx R(\omega)$. The phase of the reflected beam is related to the amplitude according to the following expression:

$$\varphi(\omega_0) = \frac{\omega_0}{\pi} \int_0^\infty \frac{\ln R(\omega)}{\omega_0^2 - \omega_0} d\omega. \tag{3}$$

The spectral dependences of the phase of the reflected beam and the absorption magnitudes in the region of excitonic resonances Γ_4 are Γ_5 are also shown in Fig. 1. It is evident from the calculated results that the phase of the reflected beam changes in the same way for both excitonic resonances, reaching the lowest values at frequencies near ω^L. A difference is observed in the contours of the absorption spectra for Γ_4 and Γ_5 excitons. For the Γ_4 excitons, the absorption maximum nearly corresponds to the transversal exciton frequency ω^T, while for Γ_5 excitons it is

shifted towards the frequency of longitudinal exciton ω^L.

The real and imaginary parts of the complex dielectric permittivity $\varepsilon_1 = n^2 + k^2$; $\varepsilon_2 = 2nk$ are determined from the calculated values of optical functions n and k of the complex refractive index. The spectral dependences of optical functions n and k, ε_1 and ε_2 for Γ_4 (Fig. 2) and Γ_5 (Fig. 3) excitons are different. Optical processes for Γ_5 excitons occur into a narrow surface region of the crystal. The optical functions of Γ_4 excitons contribute to the optical functions of the Γ_5 excitons. The second derivative of the imaginary part of dielectric constant is shown in Fig. 4 for Γ_4 and Γ_5 excitons.
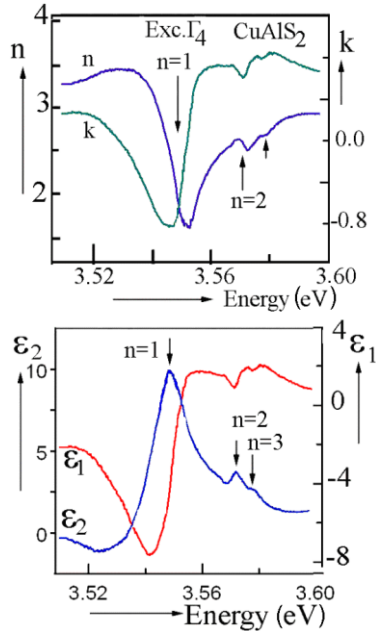

Fig. 2. Spectral dependences of optical functions n, k, ε_1, and ε_2 in the region of excitonic resonance Γ_4.
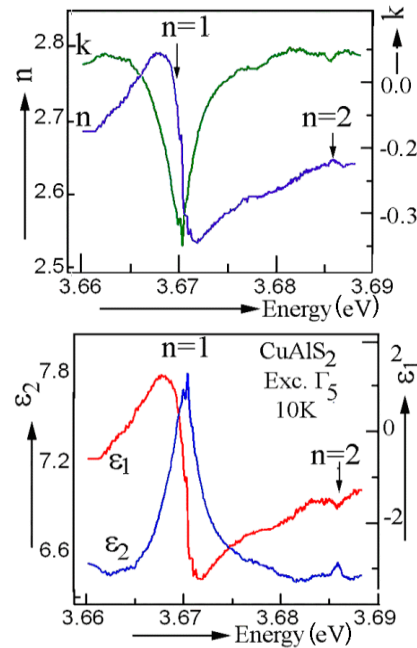
Fig. 3. Spectral dependences of optical functions n, k, ε_1, and ε_2 in the region of excitonic resonance Γ_5.

The excitonic spectra peculiarities (ground and excited excitonic states) are more evident in the derivative spectra allowing one to determine the main exciton parameters, i.e., binding energy and crystal band gap, with a higher accuracy.

The reflection spectra were measured in the depth of the fundamental absorption band in the energy interval 3–6 eV at 80 K temperature in E‖c (Fig. 5) and E⊥c (Fig. 6) polarizations. The absorption coefficient and optical functions n, k were calculated from the reflection spectra by means of Kramers−Kronig relations. Reflection maxima A_1-A_7 are observed in reflection spectra measured in E‖c polarization at a temperature of 80 K. Weak features related to Γ_4 and $\Gamma5$ excitons are also observed in these spectra. Excitonic features and B_1-B_7 maxima are observed in E⊥c polarization. The maxima observed in reflection spectra manifest themselves also in the optical functions ε_1, ε_2, $d^2\varepsilon_1/dE^2$ and $d^2\varepsilon_2/dE^2$ for E‖c (Fig. 7) and E⊥c (Fig. 8) polarizations.
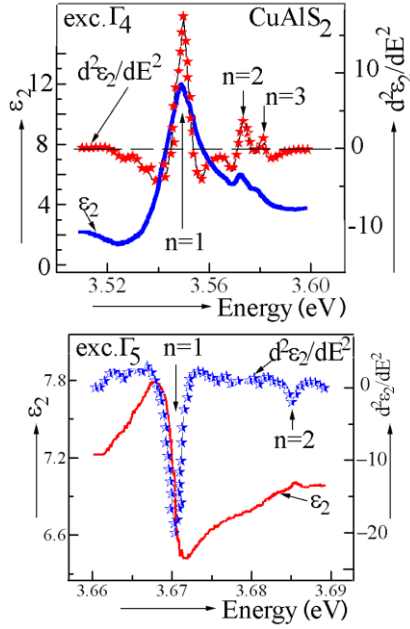
Fig. 4. Spectral dependence of ε_2 and $d^2\varepsilon_2/dE^2$ for Γ_4 and Γ_5 excitons.
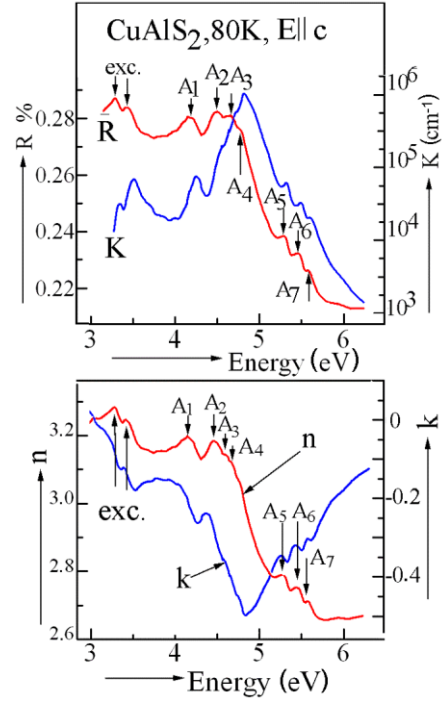

Fig. 5. Spectral dependences of reflection coefficient R and the absorption coefficient K as well as optical functions n and k calculated from reflection spectra for the $E\parallel c$ polarization.
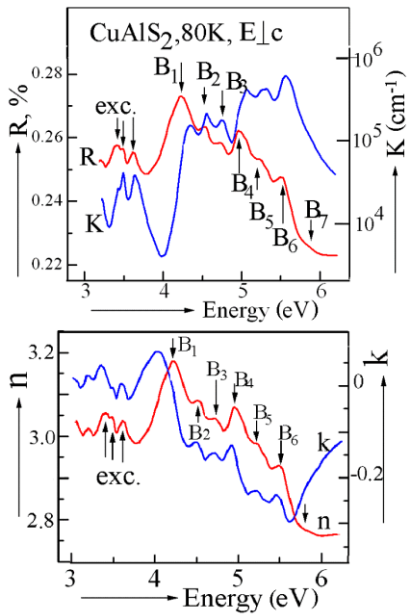

Fig. 6. Spectral dependences of reflection coefficient R and the absorption coefficient K as well as optical functions n and k calculated from reflection spectra for the $E\perp c$ polarization.
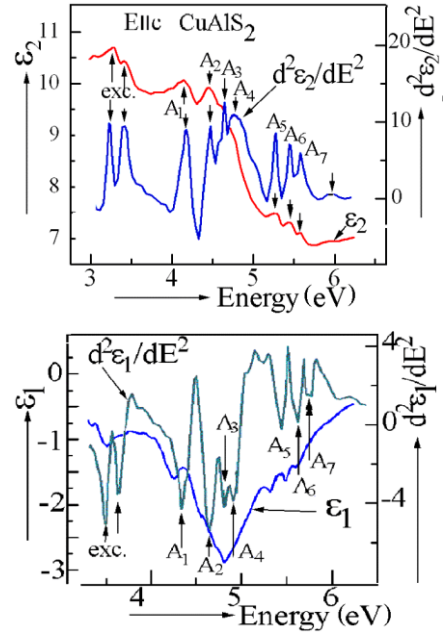

Fig. 7. Spectral dependences of optical function ε_1, ε_2, $d^2\varepsilon_1/dE^2$, and $d^2\varepsilon_2/dE^2$ calculated from the reflection coefficient R in $E\parallel c$ polarization in $CuAlS_2$ crystals.

13

Fig. 8. Spectral dependences of optical function ε_1, ε_2, $d^2\varepsilon_1/dE^2$, and $d^2\varepsilon_2/dE^2$ calculated from the reflection coefficient R in E⊥c polarization in CuAlS$_2$ crystals.
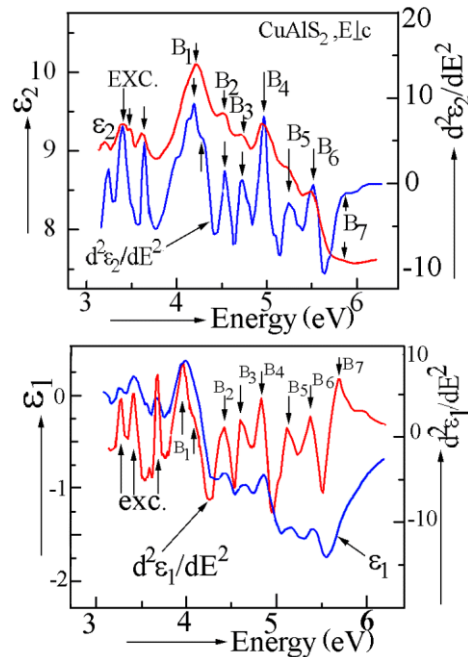
The electronic transitions revealed from experimental reflection spectra and calculation of optical functions are interpreted in the frame of theoretical calculations of crystals structure for I–III–VI$_2$ group compounds at special points T, Γ, and N of the Brillouin zone [3, 4]. Theoretical calculations of the band structure were also performed for other points of the Brillouin zone, such as Z, X, and P [5]. As mentioned by Alonso et al. [5], theoretical calculations are based on previous data [3, 4]. The results of theoretical calculations provide additional possibilities for the interpretation of experimental spectra. The theoretical calculations for CuGaS$_2$ and AgGaS$_2$ crystals [5] are very important, since they provide numeric values of interband intervals. Unfortunately, these calculations are carried out only for Γ, T, and N points of the Brillouin zone, and the interpretation of experimentally observed transitions at other specific points of the Brillouin zone is not possible on the basis of these calculations. We used numeric values of theoretical interband intervals at P, X, and Z points deduced from the energetic diagram reported by Alonso et al. [5].

The theoretical calculations of the energy band structure in the neighborhood of Z, X, and P points of the Brillouin zone are carried out without taking into account the spin-orbital interaction and the crystal field. The valence bands at these points are degenerated according to theoretical calculations. These bands are split in real crystals. This means that a bigger number of polarized excitonic transitions can be observed in reflection spectra. For instance, two upper valence bands V$_1$ and V$_2$ are revealed at the Z point of the band diagram. Each of these bands is twice degenerated. In real crystals, they are split and, as a result, four electronic transitions can occur into the C$_1$ band in a narrow energy interval in the neighborhood of the Z point. A similar situation occurs at other revealed points of the Brillouin zone. It should be mentioned that the removal of degeneracy for any of the V$_1$ bands at any point of the Brillouin zone leads to the appearance of A$_i$, E$_i$ maxima in reflection spectra.

Peculiarities related to excitonic states and maxima associated with direct electronic

transitions in the depth of absorption band are evident in the reflection spectra as well as in calculated optical functions of $CuAlS_2$ crystals (Figs. 5−8). The obtained experimental results are discussed on the basis of theoretical calculations of the band structure performed for I–III–VI$_2$ crystals by Jaffe and Zunger [3, 4]. The results of earlier and later theoretical calculations [10–12] are combined into one band diagram taking into account the energetic intervals at the special points X, P, Z, N, and T of the Brillouin zone.

We interpret the experimentally measured reflection spectra on the basis of the band diagram calculated by Alonso et al. [5]. For this purpose, a segment of the band diagram is presented in Fig. 9 in the region of the minimum interband interval. The minimal energetic interval Γ_7 (V$_1$) - Γ_6 (C$_1$) is designated as E_0. From Fig. 9, we can estimate the interband intervals at other points of the Brillouin zone compared to E_0. A similar analysis of the energy band diagram was performed for $CuGaS_2$ crystals [15]. These estimations revealed that the interband interval $\Gamma_7(V_1)$ - $\Gamma_7(C_2)$ in E_0 units is smaller than the interband intervals (V$_1$ -C$_1$) at Z, X, P, N, and T points.

According to theoretical calculations, the interband interval at the N point, namely $N_1(V_2)$ - $N_1(C_1)$ in E_0 units is significantly larger than the interband interval at the Γ point V$_1$-C$_2$. Therefore, it is more reasonable to suppose that the A$_1$, B$_1$ maxima are related to transitions at the Γ point from the V$_1$ zone to the C$_2$. A$_2$ and B$_2$ maxima are observed in the reflection spectra measured in E‖c and E⊥c polarizations, respectively, in the short wavelength region of the A$_1$, B$_1$ maxima. The energy interval between the A$_2$, B$_2$ and A$_1$, B$_1$ maxima is nearly equal to value of the valence band splitting at the center of the Brillouin zone due to crystal field and spin-orbital interaction. Taking this into account, we can suggest that A$_2$, B$_2$ maxima are also due to transitions at the center of the Brillouin zone from the $\Gamma_6(V_2)$ valence band to the $\Gamma_7(C_2)$ conduction band. The energetic interband intervals in the neighborhood of P and Z points are significantly lower as compared to those at the N point. On the basis of these results, the maxima A$_3$, B$_3$ and A$_4$, B$_4$ observed in the reflection spectra measured in E‖c and E⊥c polarizations are assigned to transitions into P and Z points, respectively, as shown in Fig. 9 and Table 1.
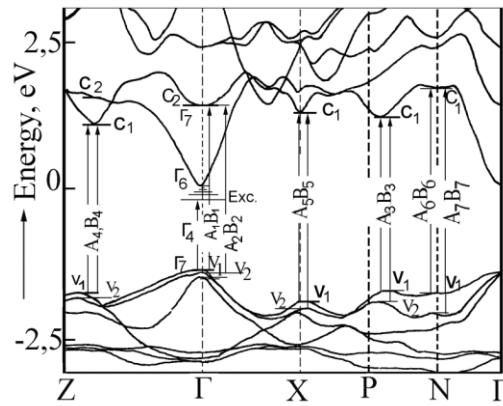

Fig. 9. Energy band structure of $CuAlS_2$ crystals.

Table 1. Electronic transitions in CuAlS$_2$crystals

Maximum	R eV	ε_2, eV	$d^2 \varepsilon_2 /dE^2$ eV	Maximum	R eV	ε_2, eV	$d^2 \varepsilon_2 /dE^2$ eV	Transition
Exc.Γ4(A)		3.575						Γ_7 - Γ_6
Exc.Γ5(B)						3.693		Γ_6 - Γ_6
Exc.Γ5(C)						3.963		Γ_6 - Γ_6
A1	4.199	4.148	4.196	B1	4.224	4.215	4.220	$\Gamma_7(V_1)$-$\Gamma_7(C_2)$
A2	4.489	4.442	4.473	B2	4.531	4.517	4.527	$\Gamma_6(V_2)$-$\Gamma_7(C_2)$
A3	4.650	4.603	4.615	B3	4.730	4.717	4.723	$P(V_1)$-$P(C_1)$, $P(V_2)$-$P(C_1)$,
A4	4.777	4.763	4.880	B4	4.971	4.959	4.963	$Z(V_1)$-$Z(C_1)$, $Z(V_2)$-$Z(C_1)$,
A5	5.290	5.273	5.254	B5	5.222	5.210	5.218	$X(V_1)$-$X(C_1)$, $X(V_2)$-$X(C_1)$,
A6	5.461	5.447	5.467	B6	5.512	5.490	5.505	$N(V_1)$-$N(C_1)$
A7	5.587	5.582	5.590	B7	5.870	5.867	5.865	$N(V_2)$-$N(C_1)$

Maxima A$_5$ (5.273 eV) and B$_5$ (5.210 eV) are observed in the reflection spectra measured in E‖c and E⊥c polarizations, respectively, in the region of 5 eV. Since the interband intervals at the X point are larger than those at the P and Z points and lower than those at the N and T points, the maxima A$_5$ and B$_5$ can be ascribed to transitions at the X point from the V$_1$ and V$_2$ bands to the C$_1$ band. Similarly, since the interband interval at the N point is larger than those at the X, P, and Z points, the maxima A$_6$ and B$_6$ revealed in the reflection spectra measured in E‖c and E⊥c polarizations, respectively, can be assigned to transitions at the N point from the V$_1$ band to the C$_1$ band, while the maxima A$_7$ and B$_7$ are also due to transitions at the N point, but from the V$_2$ band to the C$_1$ band.

4. Conclusions

The results of this study demonstrate that CuAlS$_2$ crystals possess a strong anisotropy of optical properties in the region of excitonic transitions. The parameters of Γ_4 and Γ_5 excitons were determined by Kramers-Kronig calculations of the reflection spectra, and the energy interval between the Γ_7–Γ_6, Γ_6–Γ_6 and Γ_7–Γ_6 bands were found to be of 3.575, 3.693, and 3.963 eV, respectively. The peculiarities in the reflection spectra as well as in optical functions n, k, ε_1, ε_2, $d^2\varepsilon_1/dE^2$ and $d^2\varepsilon_2/dE^2$ calculated by means of Kramers–Kronig relations were identified and ascribed to electronic transitions at various special point of the Brillouin zone taking into account the results of energy band structure calculations.

References

[1] M. V. Yakushev, A. V. Mudryi, Y. Feofanov, A. V. Ivaniukovich, and I. V. Viktorov, Thin Solid Films 511-512, 130 (2006).
[2] K. Tanaka, H. Uchiki, S. Iida, T. Terasako, and S. Shirakata, Solid State Commun. 114, 197 (2000).
[3] J. E. Jaffe and A. Zunger, Phys. Rev. B 28, 5822 (1983).

[4] J. E. Jaffe and A. Zunger, Phys. Rev. B 29, 1882 (1984).

[5] M. I. Alonso, M. Garrida, C. A. D. Rincon, and M. Leon, J. Appl. Phys. 88, 5796 (2000).

[6] M. I. Alonso, K. Wakita, J. Pascual, M. Garriga, and N. Yamomoto, Phys. Rev. B 63, 075203 (2001).

[7] N. N. Syrbu, B. V. Korzun, A. A. Fadzeyeva, R. R. Mianzelen, V. V. Ursaki, and I. Galbic, Physica B 405, 3243 (2010).

[8] N. N. Syrbu, N. D. Rabotinskii, G. I. Stratan, and S. B. Hachaturova, Fiz. Tverd. Tela 30, 865 (1988).

[9] A. M. Andriesch, N. N. Syrbu, M. S. Iovu, and V. E. Tezlevan, Physica Status Solidi (b).187, 83 (1995).

[10] S. Shirakata and S. Chichibu, J. Appl. Phys. 87, 3793 (2000).

[11] M. Susaki, N. Yamamoto, B. Prevot, and C. Schwab, Jpn. J. Appl. Phys. 35, 1652 (1996).

[12] N. Yamamoto, M. Kitakuni, and M. Susaki, Jpn. J. Appl. Phys. 34, 3019 (1995).

[13] T. Terasako, H. Umiji, K. Tanaka, S. Shirakata, H. Uchiki, and S. Isomura, Jpn. J. Appl. Phys. 38, L805 (1999).

[14] N. Tsuboi, J. Mitomo, N. Kakuda, T. Terasako, and S. Iida, Cryst. Res. Technol. 31, 341 (1996).

[15] S. Levcenko, N. N. Syrbu, V. E. Tezlevan, E. Arushanov, J. M. Merino, and M. León, J. Phys. D: Appl. Phys. 41, 055403 (2008).